

Crosstalk Analysis for Limited-Wavelength-Interchanging Cross Connects

Teck Yoong Chai, *Student Member, IEEE*, Tee Hiang Cheng, *Member, IEEE*, Sanjay K. Bose, *Senior Member, IEEE*, Chao Lu, *Member, IEEE*, and Gangxiang Shen, *Member, IEEE*

Abstract—This letter identifies crosstalk sources in limited-wavelength-interchanging cross connects (L-WIXC) and calculates the power penalty imposed by this. Specifications for the components used in the L-WIXCs can then be determined for obtaining a specified level of system performance.

Index Terms—Coherent crosstalk, limited conversion, optical cross-connect, power penalty.

I. INTRODUCTION

THE HIGH COST of wavelength converters has motivated the efficient design of optical networks that require only limited wavelength conversion capability. Studies show that full wavelength conversion may not be necessary for obtaining desirable performance levels [1], [2]. We, therefore, consider limited-wavelength-interchanging cross connects (L-WIXC), where the OXC (optical cross connect) has only a limited number of shared converters. Various studies indicate optical crosstalk to be a key consideration in designing an optical network [3], [4]. Crosstalks in some common OXC architectures have been compared in [5] with performance results given in terms of an arbitrarily defined parameter. We feel that the power penalty is a more practical performance parameter of an OXC's crosstalk performance and have used that in our analysis. Coherent and incoherent crosstalks have been considered in [6] using a Gaussian approximation, but the analysis is limited to OXCs without wavelength conversion. L-WIXCs will require special architectures for wavelength converter sharing.

Architecture I of Fig. 1 is a multistage share-per-node architecture [1]. The incoming channels are broadcast to every space switch. Each tunable filter selects one of the wavelengths. A multistage share-per-link architecture Architecture II is shown in Fig. 2. The wavelength converters here are shared on a per-link basis. This is less efficient, but allows more converters to be easily added in the same structure. The number of switches M is equal to $2W - 1$ for nonblocking operation.

Manuscript received October 9, 2001.

T. Y. Chai was with the Network Technology Research Centre, Nanyang Technological University, 639798 Singapore. He is now with Kent Ridge Digital Labs, 119613 Singapore.

T. H. Cheng and C. Lu are with the Network Technology Research Centre, Nanyang Technological University, 639798 Singapore.

S. K. Bose is with the Department of Electrical Engineering, Indian Institute of Technology, 208016 Kanpur, India.

G. Shen was with the Network Technology Research Centre Nanyang Technological University, 639798 Singapore. He is now with TRILabs Edmonton, Department of Electrical Engineering, University of Alberta, T5K 2P7 Edmonton, AB, Canada.

Publisher Item Identifier S 1041-1135(02)03225-1.

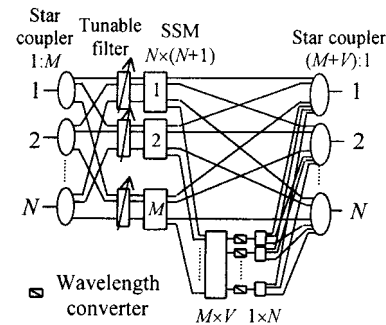


Fig. 1. L-WIXC: architecture I (SSM: Space-switching matrix).

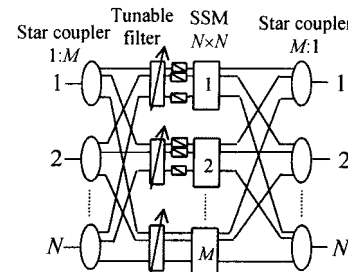


Fig. 2. L-WIXC: architecture II (SSM: Space-switching matrix).

II. THE CROSSTALK MODEL

The electrical field of a signal at center frequency ω coming from port i of an OXC may be expressed as $\vec{E}_0(t) = E b_i(t) \cos[\omega t + \phi_i(t)] \vec{P}_i$, where E is the field amplitude, $b_i(t)$ is the binary data sequence with values of zero or one in a bit period T , $\phi_i(t)$ is the phase noise of the laser, and \vec{P}_i the unit polarization vector. The signal at ω entering from port 1 is chosen as the signal in question. Here, we study inband crosstalk which has the same wavelength as the desired signal. It causes fluctuation in the signal power and is much more damaging [4]–[6].

Consider Architecture I, where $M - 1$ crosstalk components at ω leak through the filters and mix with the main signal at the star coupler, as shown in Fig. 3. Let X_i ($i = 1, 2, \dots, N$) be the number of crosstalk components at ω , leaked from the signal entering the OXC at input port i . Each X_i is then an integer satisfying $\sum_{i=1}^N X_i = M - 1$, where $1 \leq X_i \leq M - 1$. Moreover, there are $N - 1$ components at ω leaked by the first-stage switches of Fig. 3. Leakage also occurs at the last-stage switches that connect the wavelength converters and the star couplers. For a signal converted to ω , there must be another signal originally at ω being converted to another wavelength. Therefore, in the worst case, assuming V converters, there are K crosstalk components, with $K = \min(N - 1, \lfloor V/2 \rfloor)$. The converted signal

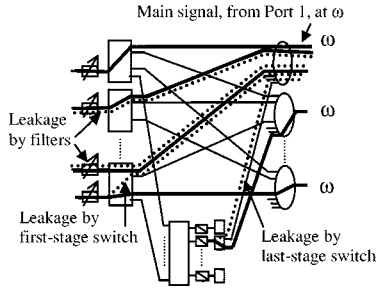


Fig. 3. Crosstalk leakage.

is free from the crosstalk carried with it before wavelength conversion. Assume that Architecture I is fully loaded and intensity modulation is used, the total electric field is given by (1) at the bottom of this page where

- $b'_i(t)$ binary data sequence of the i -th signal converted to frequency ω ;
- $\phi'_i(t)$ phase noise of the i -th signal converted to ω ;
- $\tau_{ij}, \tau_{ix}, \tau'_i$ propagation delays of the crosstalk contributions relative to the actual signal;
- $\vec{P}_{ij}, \vec{P}_{ix}, \vec{P}_i$ unit polarization vectors of the crosstalk;
- $\delta, \varepsilon, \varepsilon'$ optical power relative to the actual signal of the crosstalk contributions.

The crosstalk power penalty is defined as in [4] to be the additional power in decibel which must be added to the signal power to achieve the same error rate as that without crosstalk. Considering intensity modulation and a receiver with an integrate-and-dump filter, the decision variable is $J = \int_{nT}^{(n+1)T} |\vec{E}(t)|^2 / |\vec{E}_0(t)|^2 dt$. We assume the limits of the integration to be aligned with the bits as in a fully synchronous system. The signal noise other than the crosstalk is assumed to be Gaussian and that the crosstalk noise also approaches Gaussian behavior as the number of crosstalk sources increase [4]. If an optimal decision threshold is used [7], the power penalty pp is given by

$$pp = -10 \log [E(J) - \sigma^2 Q_0^2 / E(J)] \quad (2)$$

Here, Q_0 may be obtained from $\text{erfc}(Q_0/\sqrt{2}) = 2 \times \text{BER}$.

III. CROSSTALK ANALYSIS FOR L-WIXC

If the signal and the crosstalk are phase correlated, the crosstalk is coherent; otherwise, it is incoherent. Incoherent crosstalk components may, nevertheless interact with each other coherently to produce a composite crosstalk with much higher power [6]. The coherent effect dominates when the relative delay is less than the laser's phase coherent time, i.e., $\tau_{ij}, \tau_{ix}, \tau'_i < \text{coherent time}$. In this case, the X_i contributions leaked from the signal in the input link i in the second term of (1) will be phase-correlated. The $\phi(t - \tau)$ terms in (1) may be approximated by $\phi(t)$ to give (3), shown at the bottom of the page, where $D_{ij} = \omega\tau_{ij}$, $D_{ix} = \omega\tau_{ix}$, $D'_i = \omega\tau'_i$ and $\cos \vartheta_{ij} = \vec{P}_1 \cdot \vec{P}_{ij}$, $\cos \vartheta_{ix} = \vec{P}_1 \cdot \vec{P}_{ix}$, $\cos \vartheta'_i = \vec{P}_1 \cdot \vec{P}_i$.

- a) $\tau_{ij}, \tau_{ix}, \tau'_i \leq T$: All $b(t - \tau)$ are approximated with $b(t)$. With $\phi_1(t) - \phi_i(t)$ uniformly distributed over $[0, 2\pi]$, we have (4), shown at the top of the next page, and

$$E(J_a) = 1 + 2\sqrt{\delta} \sum_{j=1}^{X_1} \cos D_{1j} \cos \vartheta_{1j}.$$

The power penalty will be maximum when all $\cos \vartheta$ terms are equal to +1 or -1 and $X_1 = 0$. Therefore, from (2)

$$\max(pp_a) = -10 \log \left(1 - \frac{2}{3} Q_0^2 \times \left\{ \left[(M-1)\sqrt{\delta} + \sqrt{\varepsilon} \right]^2 + (N-2)\varepsilon + K\varepsilon' \right\} \right).$$

- b) $\tau_{ij}, \tau_{ix}, \tau'_i > T$: All $b(t - \tau)$ are uncorrelated with each other and with $b_1(t)$. This gives (5), shown at the top of the next page, and

$$E(J_b) = 1 + \sqrt{\delta} \sum_{j=1}^{X_1} \cos D_{1j} \cos \vartheta_{1j}$$

$$\max(pp_b) = -10 \log \left(1 - Q_0^2 \times \left\{ \frac{1}{2} \left[(M-1)\sqrt{\delta} + \sqrt{\varepsilon} \right]^2 + \frac{1}{6}(4N-7)\varepsilon + \frac{1}{6}(M-1)\delta + \frac{2}{3}K\varepsilon' \right\} \right).$$

$$\begin{aligned} \vec{E}(t) = & Eb_1(t) \cos[\omega t + \phi_1(t)] \vec{P}_1 + \sum_{i=1}^N \sum_{j=1}^{X_i} \sqrt{\delta} Eb_i(t - \tau_{ij}) \times \cos[\omega(t - \tau_{ij}) + \phi_i(t - \tau_{ij})] \vec{P}_{ij} + \sum_{i=2}^N \sqrt{\varepsilon} Eb_i(t - \tau_{ix}) \\ & \times \cos[\omega(t - \tau_{ix}) + \phi_i(t - \tau_{ix})] \vec{P}_{ix} + \sum_{i=1}^K \sqrt{\varepsilon'} Eb'_i(t - \tau'_i) \times \cos[\omega(t - \tau'_i) + \phi'_i(t - \tau'_i)] \vec{P}_i \end{aligned} \quad (1)$$

$$\begin{aligned} J \approx & \frac{1}{T} \int_{nT}^{(n+1)T} b_1^2(t) dt + \frac{2}{T} \sum_{j=1}^{X_1} \sqrt{\delta} \int_{nT}^{(n+1)T} b_1(t) b_1(t - \tau_{1j}) dt \cos D_{1j} \cos \vartheta_{1j} \\ & + \frac{2}{T} \sum_{i=2}^N \left\{ \sum_{j=1}^{X_i} \sqrt{\delta} \int_{nT}^{(n+1)T} b_1(t) b_i(t - \tau_{ij}) dt \cos[\phi_1(t) - \phi_i(t) + D_{ij}] \cos \vartheta_{ij} \right. \\ & \left. + \sqrt{\varepsilon} \int_{nT}^{(n+1)T} b_1(t) b_i(t - \tau_{ix}) dt \cos[\phi_1(t) - \phi_i(t) + D_{ix}] \cos \vartheta_{ix} \right\} \\ & + \frac{2}{T} \sum_{i=1}^K \sqrt{\varepsilon'} \int_{nT}^{(n+1)T} b_1(t) b'_i(t - \tau'_i) dt \cos[\phi_1(t) - \phi'_i(t) + D'_i] \cos \vartheta'_i \end{aligned} \quad (3)$$

$$\sigma_a^2 = \frac{2}{3} \sum_{i=2}^N \left[\left(\sqrt{\delta} \sum_{j=1}^{X_i} \cos D_{ij} \cos \vartheta_{ij} + \sqrt{\varepsilon} \cos D_{ix} \cos \vartheta_{ix} \right)^2 + \left(\sqrt{\delta} \sum_{j=1}^{X_i} \sin D_{ij} \cos \vartheta_{ij} + \sqrt{\varepsilon} \sin D_{ix} \cos \vartheta_{ix} \right)^2 \right] + \frac{2}{3} \sum_{i=1}^K \varepsilon' \cos^2 \vartheta'_i \quad (4)$$

$$\sigma_b^2 = \frac{1}{3} \delta \sum_{j=1}^{X_1} \cos^2 D_{1j} \cos^2 \vartheta_{1j} + \frac{1}{2} \sum_{i=2}^N \left(\sqrt{\delta} \sum_{j=1}^{X_i} \cos D_{ij} \cos \vartheta_{ij} + \sqrt{\varepsilon} \cos D_{ix} \cos \vartheta_{ix} \right)^2 + \frac{1}{2} \sum_{i=2}^N \left(\sqrt{\delta} \sum_{j=1}^{X_i} \sin D_{ij} \cos \vartheta_{ij} + \sqrt{\varepsilon} \sin D_{ix} \cos \vartheta_{ix} \right)^2 + \frac{1}{6} \sum_{i=2}^N \left(\delta \sum_{j=1}^{X_i} \cos^2 \vartheta_{ij} + \varepsilon \cos^2 \vartheta_{ix} \right) + \frac{2}{3} \sum_{i=1}^K \varepsilon' \cos^2 \vartheta'_i \quad (5)$$

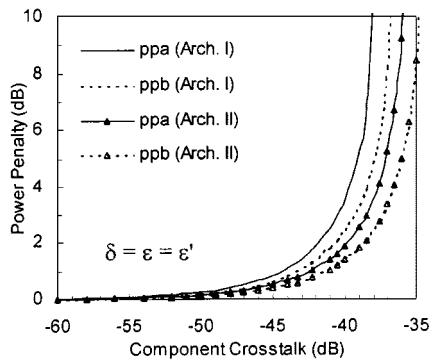


Fig. 4. Power penalty as a function of component crosstalk (BER = 10^{-9}).

Similarly for Architecture II, we derive that

$$\max(pp_a) = -10 \log \left(1 - \frac{2}{3} Q_0^2 \times \left\{ \begin{array}{l} [(M - V_n)\sqrt{\delta} + \sqrt{\varepsilon}]^2 \\ + (N - 2)\varepsilon \end{array} \right\} \right)$$

$$\max(pp_b) = -10 \log \left(1 - Q_0^2 \times \left\{ \begin{array}{l} \frac{1}{2} [(M - V_n)\sqrt{\delta} + \sqrt{\varepsilon}]^2 \\ + \frac{1}{6}(4N - 7)\varepsilon \\ + \frac{1}{6}(M - V_n)\delta \end{array} \right\} \right)$$

where V_n is the number of converters per link.

IV. RESULTS AND DISCUSSIONS

As the numerical results in Fig. 4 show, the system will have higher power penalty if the interfering bit streams are well aligned with each other (i.e., $\tau \leq T$). Under coherent crosstalk, the power penalty increases rapidly when the component crosstalk level exceeds -35 dB if the filters and the switches have the same level of crosstalk ($\delta = \varepsilon = \varepsilon'$). The crosstalk power penalty in Architecture I is higher than in Architecture II for both the cases considered. For each of the architectures, there are limits for the filter and switch crosstalk level above which a 1-dB power penalty will be impossible to achieve as indicated by Fig. 5. In the first case (pp_a), Architecture I has

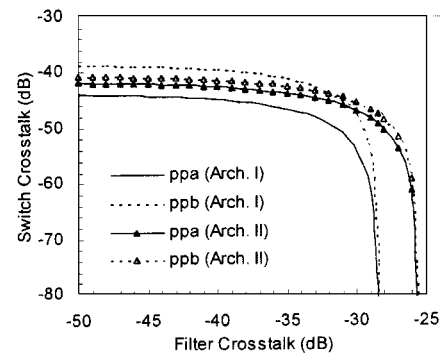


Fig. 5. Switch crosstalk as a function of filter crosstalk for $pp_s = 1$ dB.

more stringent requirement on both the filters and switches. A useful observation is that in the linear portion of the curves, a small improvement in any one of the components will significantly relax the requirements on the other kind of components.

V. CONCLUSION

The crosstalk contributions in these L-WIXCs are identified and a model is presented to quantify the impact. The results enable us to compare the performance of the L-WIXCs and to study the crosstalk requirement of the components.

REFERENCES

- [1] K.-C. Lee and V. O. K. Li, "A wavelength-convertible optical network," *J. Lightwave Technol.*, vol. 11, pp. 962–970, May–June 1993.
- [2] G. Shen, S. K. Bose, T. H. Cheng, C. Lu, and T. Y. Chai, "Operation of WDM networks with different wavelength conversion capabilities," *IEEE Commun. Lett.*, vol. 4, pp. 239–241, July 2000.
- [3] J. Zhou, M. J. O'Mahony, and S. D. Walker, "Analysis of optical crosstalk effects in multi-wavelength switched networks," *IEEE Photon. Technol. Lett.*, vol. 6, pp. 302–305, Feb. 1994.
- [4] E. L. Goldstein, L. Eskildsen, and A. F. Elrefaie, "Performance implications of component crosstalk in transparent lightwave networks," *IEEE Photon. Technol. Lett.*, vol. 6, pp. 657–660, May 1994.
- [5] T. Gyselings, G. Morthier, and R. Baets, "Crosstalk analysis of multi-wavelength optical cross connects," *J. Lightwave Technol.*, vol. 17, pp. 1273–1283, Aug. 1999.
- [6] Y. Shen, K. Lu, and W. Gu, "Coherent and incoherent crosstalk in WDM optical networks," *J. Lightwave Technol.*, vol. 17, pp. 759–764, May 1999.
- [7] H. Takahashi, K. Oda, and H. Toba, "Impact of crosstalk in an arrayed-waveguide multiplexer on $N \times N$ optical interconnection," *J. Lightwave Technol.*, vol. 14, pp. 1097–1105, June 1996.